ISBN: 978-3-95450-222-6 ISSN: 2673-5350 doi:10.18429/JACoW-IBIC2020-THPP26

TRANSVERSE BROAD-BAND IMPEDANCE STUDIES OF THE NEW IN-VACUUM CRYOGENIC UNDULATOR AT BESSY II STORAGE RING

M. Huck*, J. Bahrdt, H. Huck, A. Meseck, M. Ries
Helmholtz-Zentrum Berlin für Materialien und Energie (HZB), Berlin, Germany

Abstract

The first radiation from the cryogenic permanent magnet undulator (CPMU17) has been observed in December 2018 at BESSY II storage ring at HZB, and since then this device has served as a light source for beamline commissioning. It is the first in-vacuum undulator installed at BESSY II, and a new in-vacuum APPLE undulator (IVUE32) is planned to be installed in near future. Thus, a detailed study of the interactions between such an in-vacuum device and the electron beam is required. Beam-based measurements using orbit-bump and tune-shift methods have been applied to estimate the vertical impedance of CPMU17. For CPMU17 the first results of broad-band impedance studies are presented.

INTRODUCTION

The constantly growing requests of various research fields for synchrotron radiation with higher photon energies demands designing undulators with smaller magnetic periods and gaps. After succeeding in constructing and optimizing small gap in-vacuum undulators (IVUs) in the last two decades, the challenging impacts of such small gaps on beam dynamics can nowadays be estimated and mitigated using modern experimental techniques and high-power numerical calculations. These studies are specially required for complex structures, short bunches and variable polarization IVUs such as CPMU17 and IVUE32. One of the most important related issues is the wake fields effect. Wake fields arise when the relativistic electrons travel inside chambers with nonuniform geometrical cross-section or a resistive wall.

IMPEDANCE BY VARIABLE BEAM OFFSET AND CURRENT

A particle beam that travels off-axis through a vacuum chamber section with a nonzero broad-band transverse impedance will be deflected due to the electromagnetic forces of the wake fields generated by the particle beam itself. In frequency domain and in case of transverse impedance, such a beam-impedance interaction can be represented by a quantity called *transverse kick factor* defined by [1]

$$k_\perp = \frac{1}{2\pi}\int_{-\infty}^{\infty} Z_\perp(\omega)h(\omega)\mathrm{d}\omega, \qquad (1)$$

where $Z_\perp(\omega)$ is the frequency-dependent *transverse impedance* and $h(\omega) = \lambda(\omega)\lambda^*(\omega)$ is the bunch power spectrum, with $\lambda(\omega)$ the Fourier transform of beam linear density $\lambda(t)$. The kick factors can be calculated for both horizontal and vertical directions. However, in our studies the focus is on the kick in the vertical direction, because a small gap in-vacuum undulator comprise a flat geometry (two parallel plates), i.e. the width of the structure (46 mm in our case) is larger than its height (half gap of 3 mm-11 mm). And the interaction of the electrons with surrounding structure in the vertical direction is stronger than in the horizontal one. This interaction will cause a linear kick of the beam vertical momentum as follows

$$\Delta y' = eqk_\perp y_0/E, \qquad (2)$$

where q is the beam charge, y_0 is the beam vertical offset, E is the beam energy, and e is the electron charge. Based on Eq. (2), a method called *orbit bump method* has been developed in 1999 at Budker Institute, Novosibirsk [2] to estimate the transverse kick factor of an individual section. The closed orbit distortion (COD) due to an impedance at a section can be expressed by [1]:

$$\Delta y(s) = \frac{\Delta q}{E/e}k_\perp y_0 \frac{\sqrt{\beta(s)\beta(s_0)}}{2sin\pi Q_y} cos(|\mu(s)-\mu(s_0)|-\pi Q_y), \qquad (3)$$

where Q_y is the vertical betatron tune, $\beta(s), \mu(s)$ and $\beta(s_0), \mu(s_0)$ are respectively the betatron function and phase through the whole ring and at the location of the impedance. y_0 can be varied by introducing a closed-orbit-bump using correction coils. The orbit distortions $\Delta y(s)$ can be measured using beam position monitors (BPMs) at a high and a low beam current with a charge variation of Δq. By measuring and subtracting $\Delta y(s)$ in 4 states i.e. combination of *high-, low-current* and *with-, no-bump*: $\Delta y(s) = (\Delta y_{wbh} - \Delta y_{nbh}) - (\Delta y_{wbl} - \Delta y_{nbl})$, a COD equal to $\Delta y(s)$ is obtained which is directly proportional to $k_\perp$.

Contributions of dipole and quadrupole components in a wake field expansion have different effects on beam dynamics and can be distinguished by different measurements and models. Due to crossing terms in field expansion in a non-symmetric structure such as an IVU, $k_\perp(\omega)$ in Eq. (3) is determined with both dipole and quadrupole terms [1]. However, the quadrupole impedance manifests itself only in multi-bunch interactions [3]. The orbit bump technique is based on the *single-bunch* effect, yielding the contributions from geometric and resistive-wall broad-band dipole impedance. This technique or a variation of it has been implemented at several other institutes such as APS [4], ELLETRA [5], Diamond light source [1], Photon Factory at KEK [6], and ALBA [7].

IN-VACUUM CRYOGENIC UNDULATOR

The new in-vacuum cryogenic permanent magnetic undulator CPMU17 has been installed in summer 2018 at BESSY

* maryam.huck@helmholtz-berlin.de

ISBN: 978-3-95450-222-6 ISSN: 2673-5350 doi:10.18429/JACoW-IBIC2020-THPP26

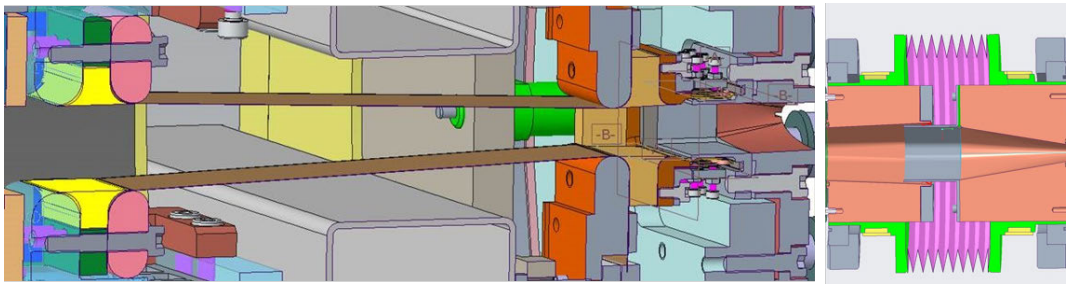

Figure 1: Schematics of the vacuum components inside the CPMU17 undulator chamber, including the tapered part and the taper section (left), and a bellow with an extra tapered octagon-ellipse transition part at ID down- and upstream (right).

II, and in fall 2018 the first undulator radiation from this device was detected. The characterization and implementation of this device has been presented in [8]. In order to reduce the geometrical discontinuities, the magnets are covered with a two layer RF-shielding foils made of Copper and Nickel. The 50 µm Copper is coated on a 50 µm thick Nickel foil. The Nickel side is attracted by magnetic forces whereas the Copper side faces the electron beam. The choice of Copper is to reduce the resistive impedance of the device. Furthermore, due to the small skin depth of Copper especially at high frequencies, electromagnetic radiation does not penetrate deeply into the Copper and will be damped in the first 0.6 µm of its surface at 10 GHz and 6 µm at 100 MHz. Another foil made of a Copper-Beryllium alloy connects the magnet part to the taper section (Fig. 1). The special construction of the taper section (Fig. 2) enables a variable taper which at one end has a fixed height of 11 mm and at the other end has a height equal to the variable magnetic gap. Down- and upstream the ID, there are bellows with cooled Copper tubes with variable cross section inside, both for the purpose of heat transport and for RF shielding the bellow discontinuities. Along the bellow, the wall cross-section is tapered from elliptical shape to an octagonal one, and there are two such transitions at either sides of the CPMU17 and two more at either sides of the UE48 (another ID downstream the CPMU17).

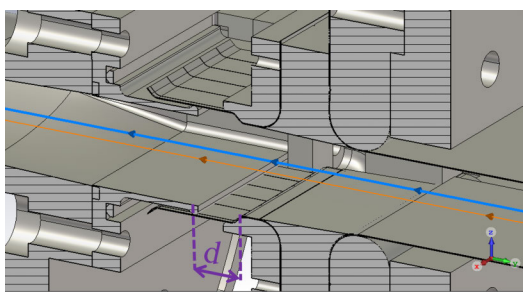

Figure 2: CAD model of the taper section used for the CST simulations.

CST Simulation

The taper section enables a variable tapering system to reduce the geometrical impedance, but it also introduces small discontinuous regions which might cause RF resonances inside the structure. The effects of this issue on wake fields has been estimated [9] using the wake field solver of the CST studio-suite simulation tool [10], and been taken into account during the design of the ID. Simulation showed, that the electromagnetic power deposited by the beam on the structure increases at larger distances of d shown in Fig. 2 [9], as do the kick factors. In operational cooled state $d \approx 2.35$ mm at 6 mm gap, and $d \approx 3.35$ mm at 22 mm. Preliminary simulation results for the taper section, tapered part and magnet part with resistive Cu foils at gap of 6 mm suggests a total kick factor of $k_y \approx 2 \times 10^{14}$ V/C/m. The contribution of the 4 bellows, 3 BPMs, and the other vacuum components and resistive walls should be added to this value. For this simulation, a rms bunch-length of $\sigma = 8.4$ mm and a beam charge of 8×10^{-9} C is used and the simulation follows the approach described in [11, 12] and used in [13].

BEAM BASED MEASUREMENTS

Two different beam-based methods are used to study the short-range wake fields of the CPMU17. One measurement used the orbit bump method and the other one vertical betatron tune-shift with bunch current change, both with a single bunch electron beam.

Orbit Bump Measurement

For this measurement the storage ring current was switched to low current already 3 hours prior to measuring CODs, reducing obit drift due to the temperature changes

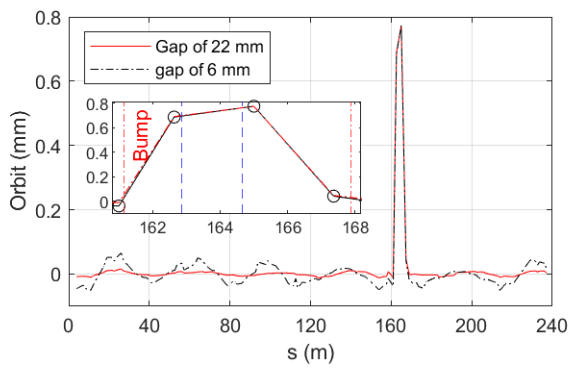

Figure 3: Vertical orbit bump at gap of 22 mm and 6 mm. The inset figure shows the bump shape closer; vertical blue lines show the place of the CPMU17 and the circle datapoints shows the position of the 3 BPMs within the bump.

ISBN: 978-3-95450-222-6 ISSN: 2673-5350 doi:10.18429/JACoW-IBIC2020-THPP26

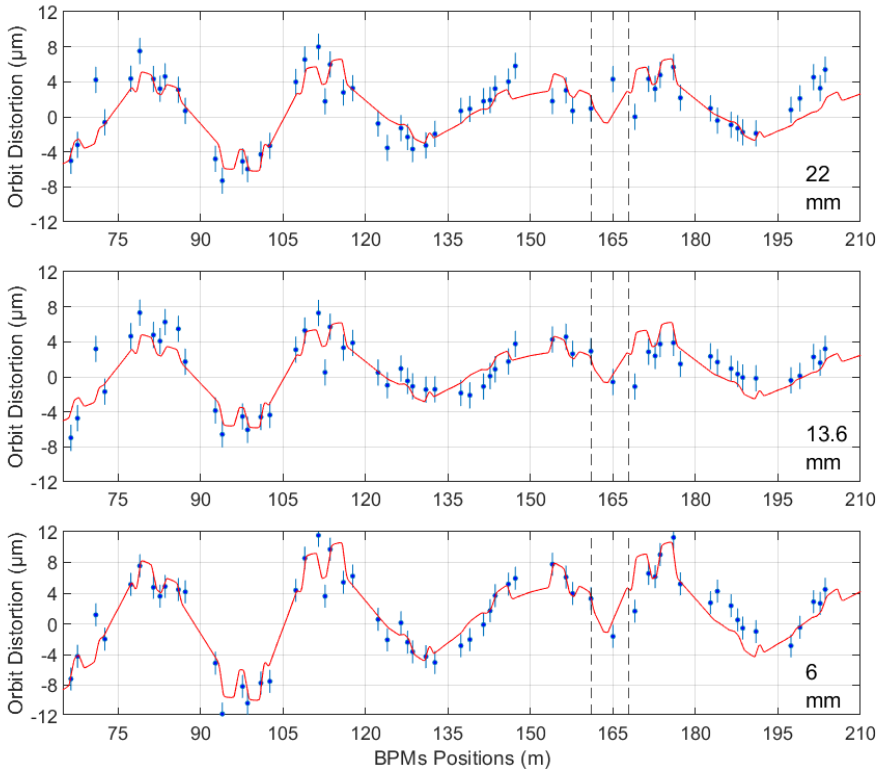

Figure 4: Three examples of closed orbit distortion $\Delta y(s)$ at gap of 22 mm, 13.6 mm and 6 mm, respectively from top to bottom. The longitudinal positions of the bump in ring is marked with vertical dashed black lines at 161.1 (downstream) and 167.9 m (upstream). The ID in ring is located between 162.87 m and 164.67 m.

of the machine. The orbit- and tune-feedback systems were turned off, but the tune feed-forward was still applied. A bump was generated using 4 steerers covering a section over a total length of about 6.4 m. The height of the bump was restricted by the machine protection system to about 0.8 mm. Two example bumps at gap of 22 mm and 6 mm are shown in Fig. 3. The bump was optimized at the gap of 22 mm with almost no disturbance outside the bump, but at the other gaps, a distortion of up to 50 μm has been observed. The amplitude of this distortion increases by decreasing the gap. This behavior was expected due to strong focusing effects while the steerers remain constant. The beam used for the measurement was a single bunch with a beam current of 4 mA and 16 mA, (low- and high-current states); corresponding to a charge difference of $\Delta q = 9.6 \times 10^{-9}$ C and an average charge of 8.0×10^{-9} C.

Three example CODs at gaps of 22 mm, 13.6 mm and 6 mm are shown in Fig. 4. In these graphs, the blue dots show average values of 18 measurements taken for 36 seconds. The standard deviation of the BPM signals over this period of time was very close to zero, the accuracy is about 1.5 μm. The red solid line is the orbit deviation calculated using the Eq. (3). It can be seen, that the amplitude of the COD at gap of 13.6 mm has the smallest value among the three, and it increases with increasing or decreasing the gap. This is a reasonable trend, because the height of the following section is 11 mm. Hence, the tapered part is flat at a gap with a height closer to this value and the impedance is the smallest. Determining the exact kick-factor minimum needs more detailed studies at gaps around 11 mm.

A fit of the measured data with the theoretical formula in Eq. (3) yields kick factors of $(6.8 \pm 0.4) \times 10^{14}$ V/C/m, $(4.0 \pm 0.3) \times 10^{14}$ V/C/m, and $(4.2 \pm 0.4) \times 10^{14}$ V/C/m, respectively at the gaps of 6 mm, 13.6 mm, and 22 mm. They are calculated excluding BPMs at longitudinal position from zero (70 m downstream the bump) to 64 m; At this area, there are obvious phase discrepancies between the measured data and the theory at gaps larger than 6 mm. Possible source for this discrepancies could be the ID focusing-effects on betatron function and phase, and linear optics-distortion due to the gap variation, not taken in to account in these analyses. Used parameters are a vertical betatron tune of $Q_y = 6.726$, a beam energy of 1.7 GeV, an average bump height of 0.73 mm measured with respect to the mechanical aperture of the U17, and an over the bump length averaged betatron phase and function of $\mu(s_0) = 28.7$ rad and $\beta(s_0) = 1.65$ m at the location of CPMU17. Because inside the undulator the beta function has a very small variation (Fig. 5), a constant value for $\beta(s_0)$ in Eq. (2) has been used. The vertical betatron function at the straight section of CPMU17 was (already before the installation) adjusted to low values with a local lattice modification to exclude a fatal beam scraping at the magnetic structure [14]. Installing an IVU in such a mini-beta section implies the advantage that the beam orbit will have less distortion due to the wake fields according to Eq. (3). The phase advance along the ID was 1.21 rad, less than 1π;

ISBN: 978-3-95450-222-6 ISSN: 2673-5350 doi:10.18429/JACoW-IBIC2020-THPP26

this condition is required for using the orbit bump method, so that the sections with the same impedance and with a phase difference of π do not lead to zero orbit deviations outside the bump [1, 2].

A length of 1.8 m inside the bump region is already covered by the undulator itself, and in the rest of the region there is not any significant geometrical discontinuities which could contribute to the measured impedance. The major sources of the geometrical and resistive wakes in this region lies within the undulator itself, mainly at the taper section, the tapered part and also four tapered transition parts shown in Fig. 1, and 3 BPMs within the bump.

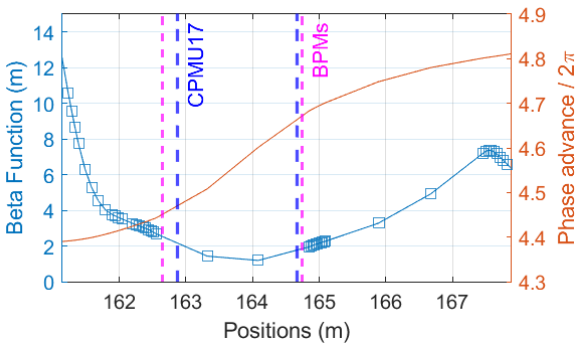

Figure 5: Vertical betatron function and phase advance within the bump. Dashed lines display the location of CPMU17 and its surronding BPMs.

Tune Shift Measurement

In our second studies, the variation of the vertical betatron tune was measured vs. single bunch current change. The slope of this variation is an indication of the *vertical dipolar kick factor* $k_\perp$ according to the following equation [5, 13, 15, 16]:

$$\frac{dQ_{yF}}{dI_b} = -\frac{<\beta> k_\perp}{4\pi\nu_{rev}(E/e)}, \qquad (4)$$

where I_b is the bunch current, $\nu_{rev} = 1.249\,\text{MHz}$ is the revolution frequency, Q_{yF} is the coherent *fractional vertical tune* [15], and E is the beam energy. Both dipole and quadrupole wakes contribute to the coherent tune shift, but theoretically the quadrupole term is smaller than the dipole one, and it can be detected by introducing quadrupole field oscillations [15].

We used conventional strip-line kickers to induce vertical dipolar oscillations, and the vertical fractional tune-shift was measured using the beam diagnostics system for two cases with ID open and closed. The tune feedback system was off, while the tune feed-forward table, for compensating the undulator focusing effect, was still applied. This table corrects the gap-dependent vertical tune-shift of about $\Delta\nu_y = 2.8\,\text{kHz}$ (moving from gap of 22 mm to 6 mm) with an accuracy of about $d\nu_y = \pm 0.7\,\text{kHz}$. The resolution of the betatron frequency measurement was $d\nu_y = 140\,\text{Hz}$ (rms of the statistical errors). At each current, the betatron frequency was measured for several times and averaged (Fig. 6). The slopes of the linear fits are

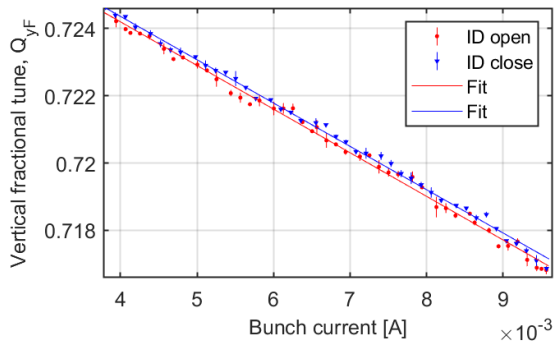

Figure 6: Tune shift by current change. Dots are the measured data with statistical errors, solid lines are linear fits.

$(-1.2864 \pm 0.076)\,\text{A}^{-1}$ and $(-1.2954 \pm 0.011)\,\text{A}^{-1}$, respectively at closed and open gaps, resulting in a slope difference of $(9.1 \pm 13.6) \times 10^{-3}\,\text{A}^{-1}$ between the two cases. By substituting this value in Eq. 4, we get a kick value of $(1.5 \pm 2.2) \times 10^{14}$ V/C/m. The large error shows, that the contribution of the CPMU17 to the total dipole vertical kick-factor of BESSY II is too small, to be resolved by this measurements accuracy. Applying the difference of kick factors at open and closed ID derived by the OBM method above, $\Delta k_y = (2.6 \pm 0.5) \times 10^{14}$ V/C/m to Eq. (4), slope difference of $(16 \pm 3) \times 10^{-3}\,\text{A}^{-1}$ is deduced which corresponds to a tune change of $dQ_{yF} = (1.5 \pm 0.6) \times 10^{-5}$ (when the bunch current sweeps by 1 mA). Hence, a betatron frequency change of $d\nu_y = (20 \pm 4)$ Hz is expected, for which a measurement accuracy in the same order is required.

CONCLUSION

The major impedance contributors of the first cryogenic permanent undulator at BESSY II have been identified, and the impact of the taper section, magnets-shielding and tapered foils on the impedance have been separately approximated using CST simulations. The vertical kick factors have been experimentally evaluated using orbit-bump and tune-shift techniques. The two measurement methods and preliminary simulation results agree to a good extent. Further studies with more accurate measurements, data analyses, simulations and theoretical models are being carried out, to determine and compare the contributions of all ID parts to the impedance. Furthermore, a modification of the vacuum chamber is under development to investigate possible resonances by installing RF antennas in ID vacuum chamber. In addition, studies of coupled bunch instabilities, in particular growth-damp measurements are planned. The impedance evaluation will be also conducted with few-bunch and multi-bunch fill patterns.

ACKNOWLEDGMENTS

The author would like to acknowledge with much appreciation O. Tanaka (KEK), V. Smaluk (BNL), B. Salvant (CERN), V. Dürr, D. Wolk, S. Grimmer, T. Schroeter, T. Flisgen, W. Frendtrup, M. Scheer, S. Liangliang, and H.W. Glock (HZB) for their help and support.

ISBN: 978-3-95450-222-6 ISSN: 2673-5350 doi:10.18429/JACoW-IBIC2020-THPP26

REFERENCES

[1] V. Smaluk, R. Fielder, A. Blednykh, G. Rehm, and R. Bartolini, "Coupling impedance of an in-vacuum undulator: Measurement, simulation, and analytical estimation", *Phys. Rev. ST Accel. Beams*, vol. 17, p. 074402, 2014. doi:10.1103/PhysRevSTAB.17.074402

[2] V. Kiselev and V. Smaluk Budker Institute of Nuclear Physics, "A method for measurement of transverse impedance distribution along storage ring", in *Proc. DIPAC'99*, Chester, UK, May 1999, paper PT19, pp.202–204.

[3] A. Blednykh, G. Bassi, Y. Hidaka, and V. Smaluk, "Low-frequency quadrupole impedance of undulators and wigglers", *Phys. Rev. Accel. Beams*, vol. 19, p. 104401, 2016. doi:10.1103/PhysRevAccelBeams.19.104401

[4] L. Emery, G. Decker, and J. Galayda, "Local Bump Method for Measurement of Transverse Impedance of Narrow-Gap ID Chambers in Storage Rings", in *Proc. 19th Particle Accelerator Conf. (PAC'01)*, Chicago, IL, USA, Jun. 2001, paper TPPH070, pp.1823-1825.

[5] E. Karantzoulis, V. Smaluk, and L. Tosi, "Broad band impedance measurements on the electron storage ring ELETTRA", *Phys. Rev. ST Accel. Beams*, vol. 6, p. 030703, 2003. doi:10.1103/PhysRevSTAB.6.030703

[6] O. A. Tanaka *et al.*, "Evaluation of the Transverse Impedanse of Pf in-Vacuum Undulator Using Local Orbit Bump Method", in *Proc. 7th Int. Beam Instrumentation Conf. (IBIC'18)*, Shanghai, China, Sep. 2018, pp. 89–92. doi:10.18429/JACoW-IBIC2018-MOPB08

[7] Z. Martí, G. Benedetti, T. F. G. Günzel, and U. Iriso, "Local Impedance Measurements Using the Orbit Bump Method at ALBA", in *Proc. IPAC'19*, Melbourne, Australia, May 2019, pp. 240–242. doi:10.18429/JACoW-IPAC2019-MOPGW066

[8] J. Bahrdt *et al.*, "Characterization and Implementation of the Cryogenic Permanent Magnet Undulator CPMU17 at Bessy Ii", in *Proc. IPAC'19*, Melbourne, Australia, May 2019, pp. 1415–1418. doi:10.18429/JACoW-IPAC2019-TUPGW014

[9] Thomas Flisgen, "Internal report on CPMU17 impedance studies", HZB, Berlin, Germany, 2018, unpublished.

[10] Computer Simulation Technology (CST), CST Studio Suite, particle dynamics, accelerator components, cavities, wake fields, https://www.3ds.com/products-services/simulia/products/cst-studio-suite/solvers/

[11] Benoit Salvant, "Transverse single-bunch instabilities in the CERN SPS and LHC", presented at Beam physics for FAIR Workshop, Bastenhaus, Germany, Jul. 2010.

[12] C. Zannini, "Electromagnetic simulation of CERN accelerator components and experimental applications", Ph.D. Thesis, Phys. Dept., Ecole Polytechnique Federale de Lausanne, Lausanne, Switzerland.

[13] O. A. Tanaka *et al.*, "Impedance evaluation of in-vacuum undulator at KEK Photon Factory", *J. Phys.: Conf. Ser.*, vol. 1067, p. 062008, 2018. doi:10.18429/JACoW-IPAC2018-THPAK001

[14] J. Bahrdt *et al.*, "Measurements of the Lattice Modifications for the Cryogenic Undulator CPMU17", in *Proc. IPAC'16*, Busan, Korea, May 2016, pp. 4031–4034. doi:10.18429/JACoW-IPAC2016-THPOW039

[15] S. Sakanaka, T. Mitsuhashi, and T. Obina, "Observation of transverse quadrupolar tune shifts in the Photon Factory storage ring", *Phys. Rev. ST Accel. Beams*, vol. 8, p. 042801, 2005. doi:10.1103/PhysRevSTAB.8.042801

[16] T. F. Günzel, "Coherent and Incoherent Tune Shifts Deduced from Impedance Modelling in the ESRF-Ring", in *Proc. EPAC'04*, Lucerne, Switzerland, Jul. 2004, paper WEPLT083, pp. 2047–2049.